FDTD based efficient 2D simulations of Indoor propagation for wireless LAN.

J.M. Gorce, K. Runser, G. de la Roche

CITI ; ARES-INRIA

INSA Lyon

Villeurbanne, 69621 France

Phone: +33-4-72-43-60-68, Fax: +33-4-72-43-62-27, E-mail: jean-marie.gorce@insa-lyon.fr

Abstract - This paper describes and evaluates a new algorithm for the purpose of Indoor propagation prediction for centimetric waves. Usual approaches previously developed for Indoor propagation are based either on empiric or ray-tracing technics. The former suffers a lake of accuracy while the later offers the possibility of a trade-off between accuracy and computation load. Ray-tracing has been shown really efficient for urban or semi-open environments for those few diffraction and reflection steps have to be taken into account for a specific ray. On the contrary, in severe Indoor environments, multiple diffraction and reflections reduce the quality of ray-tracing predictions. In this work, our goal is to propose an alternative to the very popular ray-tracing approach. The starting point of our approach is the use of an accurate algorithm and then the development of an efficient algorithm to reduce the computation load. Our approach started from a formalism similar to the famous TLM approach in the frequency domain. Since the problem reduces to a linear system problem, we investigate the potential of a multi-resolution approach to solve it with a lower complexity than standard time-domain TLM algorithms.This method may be considered as a boundary value problem, and has a strong similitude with the Minimum Autonomous Bloc method. The originality of our work is the way that the propagation is computed over a multi-resolution tree architecture, referring encapsulated bricks on which the propagation is recursively computed. This architecture is well adapted for the design of a wireless LAN.

Keywords— **Frequency domain TLM, Indoor propagation, wLAN planning, multi-resolution algorithm.**

I. INTRODUCTION

During the two last decades, lot of softwares have been developed to help telecommunication operators to develop their radio networks. The problem hardness depends on the wave frequency, the network size and the propagation environment [NES 00]. With the very fast deployment of cellular phone systems, the main efforts were first dedicated to outdoor applications. In this context, the high size of environments was such that empiric methods were often preferred. Later, the fast increase of deployed radio cells in urban areas called for more specific methods taking into account more precisely the geometry of the cells. Deterministic methods were then widely proposed, developed in a geometrical optic framework and using extensively the unified theory of diffraction (UTD), providing a wide range of methods (e.g. ray-tracing, ray launching, ray tube based algorithms). During the last decade a more attention was paid to Indoor environments [CHE 97], [VAL 93], [LU 04], firstly for DECT networks and for Indoor micro-cells for

cellular networks, and more recently to face the exponential growing of the deployment of WiFi like wireless LAN (wLAN). In many cases, Indoor environments are severe because of the high number of reflections or diffractions occurring when the wave propagates through offices, corridor and floors. More recent works have been devoted to the extension of ray-tracing approaches toward true three-dimensional versions, and to improve the way the diffraction is taken into account. However, increasing the accuracy of these approaches implies the drastic increase of the computation load. Though, wLAN planning requires numerous simulations for different acces point (AP) locations, and thus needs fast computation of AP's coverage area. Thus, in practical situations wLAN engineers prefer to reduce the complexity of ray-tracing by limiting ray paths about 3 segments. Our work was guided by this fact, and the algorithm we developed was expected to propose an accurate but fast technic to compute the wave propagation.

The choice of the method is justified in three points :

• First, the choice was oriented to FDTD like methods in order to ease the simulation of reflection and diffraction effects.

• Second, considering that in WiFi applications time spreading is small, a steady state prediction was expected to be enough, allowing the use of a frequency domain approach.

• Third, the ParFlow theory [LUT 98] has been selected for its simplicity and its equivalence with the TLM theory.

The constraint of a low computation load leads to the following statements :

• The problem is studied in a restricted two-dimension (2D) space.

• Because lot of possible radio Access Point locations (wave source) have to be assessed, it appears interesting to propose a way to solve the problem in two steps: the former corresponding to a pre-processing phase, disregarding the source location, the later allowing to assess the coverage of a source in a time as short as possible.

SectionII presents the ParFlow theory. SectionIII presents implementation aspects and section IV gives some results and details how this approach is used in a network planning framework.
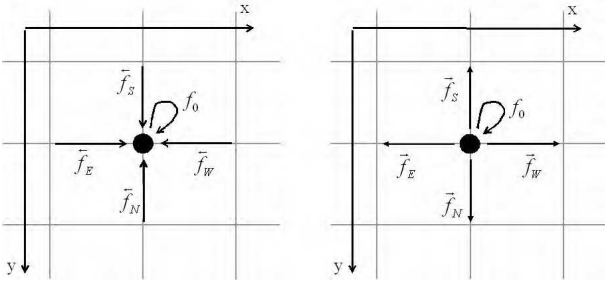
Fig. 1. 5 inward flows (a) and 5 outward flows (b) are associated with each pixel.

II. THE PARFLOW THEORY

In this section, the Frequency-Domain ParFlow (FDPF) method is presented. First, the basic ParFlow theory is introduced and then the multi-resolution approach in the frequency domain is presented. For the sake of simplicity, the problem is addressed in 2D for the transverse electric field component only. The approach could be nevertheless easily extended to a 3D formulation, but this is not assessed herein because it would lead to a too high computation load in our application framework.

A. Time-Domain ParFlow

The time domain ParFlow theory has been proposed by Luthi [LUT 98] from a Lattice Boltzmann formalism. Its application in the context of cellular network planning has been investigated in [CHO 97].

In the ParFlow approach [CHO 97], the electric field is settled in 5 components, 4 directive flows bringing each one energy toward the associated cardinal direction and an additional inner flow. These flows are driven by local transition matrices derived from the Maxwell's equations. [LUT 98]. In this paper, these flows are referred to as $\overleftarrow{f_d}$ and $\overrightarrow{f_d}$ respectively for inward and outward flows, where the index $d, (d \in \{E, W, S, N, 0\})$ indicates the direction of each flow (East, West, South, North, and 0 for the inner flow). The inner flow f_0 has been introduced [LUT 98] to simulate simultaneously different dielectric media ($\epsilon_r \neq 1$). These 5 flows are shown in Fig.1. Having a mesh of N_r rows and N_c columns, let the inward and outward flow vectors be defined by:

$$
\overleftarrow{F}(m,t) = \begin{bmatrix} \overleftarrow{f_E}(i,j,t) \\ \overleftarrow{f_W}(i,j,t) \\ \overleftarrow{f_S}(i,j,t) \\ \overleftarrow{f_N}(i,j,t) \\ \overleftarrow{f_0}(i,j,t) \end{bmatrix} \; ; \quad \overrightarrow{F}(m,t) = \begin{bmatrix} \overrightarrow{f_E}(i,j,t) \\ \overrightarrow{f_W}(i,j,t) \\ \overrightarrow{f_S}(i,j,t) \\ \overrightarrow{f_N}(i,j,t) \\ \overrightarrow{f_0}(i,j,t) \end{bmatrix} \quad (1)
$$

Beside, $\Psi(\mathbf{i}, \mathbf{j}, \mathbf{t})$ is the solution of the wave equations if the flows are driven by:

$$
\overrightarrow{F}(m,t) = \Sigma(m) \cdot \overleftarrow{F}(m, t - dt)
$$

$$
\overleftarrow{F}(m,t) = N(\overrightarrow{F}(m,t)) + S(m,t)
$$

$$(2)$$

where
$S(m,t) = [s_0(m,t), s_0(m,t), s_0(m,t), s_0(m,t), 0]^t$
is the radiating source positioned at node m, and $\Sigma(m)$ is the local scattering matrix [CHO 97], [GOR 01].

$N(\overrightarrow{F}(m))$ is the vector of neighbor outward flows toward the current pixel :

$$
N(\overrightarrow{F}(m)) = \begin{bmatrix} \overrightarrow{f_E}(i-1,j,t) \\ \overrightarrow{f_W}(i+1,j,t) \\ \overrightarrow{f_S}(i,j-1,t) \\ \overrightarrow{f_N}(i,j+1,t) \\ \overrightarrow{f_0}(i,j,t) \end{bmatrix} \quad (3)
$$

Chopard et al. [CHO 97] have used a cellular automata to solve the ParFlow equations. They have shown that such a formalism takes into account implicitly losses, reflection, and diffraction effects. In fact and as pointed out by Chopard himself, this approach is similar to the usual TLM approach used for electronic circuits and antennas design (see for instance [JOH 87], [REB 99]), although the theoretical foundation is issued from a Lattice Boltzmann formulation.

When compared to ray-tracing, the Parflow method may suffer from its slowness. Indeed, a high computation time is needed to get the radio coverage over a large space such as a building floor. This high computation load is inherent to all FDTD methods, due to the high resolution required. For the ParFlow approach, we have [CHO 97]:

$$
dr = c_0 \sqrt{2} \cdot dt \quad (4)
$$

This relation warrants that the solution of the problem corresponds to physical waves. Note that higher is the spatial resolution, better is the accuracy, but in turn larger is the mesh size and so higher is the computation load. A limit has been empirically proposed in [CHO 97] which states that the spatial resolution should be at least 6 times lower than the wavelength :

$$
dr \leq \lambda/6 \quad (5)
$$

Moreover, the iteration number should equals several times the mesh size in order to take into account an important multi-path phenomenon in Indoor environments.

B. Frequency Domain ParFlow

The translation of the TLM problem into the frequency domain is well-known for characterizing resonators in circuit

design [HES 02] and to evaluate circuits or antennas behavior in steady state. The frequency domain approach has been more rarely proposed in the context of wireless network planning [GOR 01], [GOR 03].

In this approach the problem is solved only for a specific frequency ν_0 equals to the carrier frequency and leads to a steady-state study. By this way the complexity of the problem is reduced and leads to a linear problem. To address the task of radio coverage prediction, such an harmonic steady-state study could be stated as inappropriate because fading effects cannot be estimated. However, it seems realistic to considere that the time spreading of the radio channel in Indoor environments at 2.4GHz or 5GHz is small enough compared to the duration of WiFi-like pulses. The radio channel can be therefore assumed to be not time dispersive and the harmonic response is enough to describe the radio channel.

The inner flow introduced in the time-domain formulation acts as the stub introduced in TLM theory: the aim is to overcome the time synchronism and to allow different media to be simultaneously simulated. In this way, reflection and diffraction effects are obtained. In the frequency domain this additional variable is no longer necessary and can be directly introduced by setting accordingly the scattering matrix coefficients. The local scattering matrix in the frequency domain becomes [GOR 05]:

$$\Sigma(m) = \sigma_0 \cdot \begin{bmatrix} \sigma_1 & \sigma_2 & \sigma_1 & \sigma_1 \\ \sigma_2 & \sigma_1 & \sigma_1 & \sigma_1 \\ \sigma_1 & \sigma_1 & \sigma_1 & \sigma_2 \\ \sigma_1 & \sigma_1 & \sigma_2 & \sigma_1 \end{bmatrix} \tag{6}$$

where σ_0, σ_1 and $sigma_2$ are spatially varying and depend on the constitutive material of pixel m, through two fundamental parameters : the attenuation factor $\alpha(m)$ and the refraction index $n(m)$.

New notations are then used to describe the problem for nodes at the floor level (level 0) in the pyramid (introduced below). The flows are :

$$\overleftarrow{F}^0(m) = \begin{bmatrix} \overleftarrow{f_E}(m) \\ \overleftarrow{f_W}(m) \\ \overleftarrow{f_S}(m) \\ \overleftarrow{f_N}(m) \end{bmatrix} \quad ; \quad \overrightarrow{F}^0(m) = \begin{bmatrix} \overrightarrow{f_E}(m) \\ \overrightarrow{f_W}(m) \\ \overrightarrow{f_S}(m) \\ \overrightarrow{f_N}(m) \end{bmatrix} \tag{7}$$

The flows obey locally to the following bounds:

$$\overrightarrow{F}(m) = \Sigma(m) \cdot \overleftarrow{F}(m)$$

$$\overleftarrow{F}(m) = N(\overrightarrow{F}(m)) + S(m) \tag{8}$$

These local equations can be written in a unique global equation if the unknowns are gathered into a unique vec-

tor according to

$$\underline{\overleftarrow{F}}^0 = [\overleftarrow{F}^0(0), \overleftarrow{F}^0(1), \ldots, \overleftarrow{F}^0(m) \ldots, , \overleftarrow{F}^0(M-1)]^t$$

$$\underline{S}^0 = [S^0(0), S^0(1), \ldots, S^0(m), \ldots, S^0(M-1)]^t$$

$$\tag{9}$$

leading to the following equation:

$$\left(I_d - \underline{\Omega}^0\right) \underline{\overleftarrow{F}}^0 = \underline{S}^0 \tag{10}$$

where I_d is the identity matrix and $\underline{\Omega}^0$ is the propagation matrix.

At this point, the original ParFlow method has been translated into the frequency domain leading to a linear system. Even with special inversion algorithms for sparse matrices, this resolution becomes rapidly unbearable as the environment size increases and especially on a standard computer. For instance an environment of 1000×1000 such as a floor of $100m \times 100m$ at a resolution of $10cm$ would require the inversion of a sparse matrix of size $(4 \cdot 10^6 \times 4 \cdot 10^6)$. As described in [GOR 05], (10) can be solved efficiently when derived as the sum of a geometric series

$$\underline{\overleftarrow{F}}^0 = \sum_{k=0}^{\infty} \left(\underline{\Omega}^0\right)^k \cdot \underline{S}^0 = \underline{S}^0 + \underline{\Omega}^0 \cdot \underline{S}^0 + \left(\underline{\Omega}^0\right)^2 \cdot \underline{S}^0 + \ldots$$

$$\tag{11}$$

Propagation is then computed with the following algorithm

Algorithm II.1

Initialization : $\forall m, \forall d$, set $f_m^d = s_0$.
  at the source node $m_s, \forall d$, set $f_{m_s}^d = s_0$.
Do *(until stability is reached)*
  Set incoming flows:
    $\forall m, \overleftarrow{F}^0(m) = N(\overrightarrow{F}^0(m))$
  Accumulate :
    $\forall m, \overleftarrow{F}^{acc}(m) = \overleftarrow{F}^{acc}(m) + \overleftarrow{F}^0(m)$
  Set outward flows :
    $\forall m, \overrightarrow{F}^0(m) = \Sigma^0(m) \cdot e^{-j2\pi\nu dt} \cdot \overleftarrow{F}^0(m)$
Until convergence

Note that only very few differences hold when compared to the usual time domain algorithm.

Since an harmonic mode is studied, the steady-state is reached when the electric field is stationary. A whole time-spreading response of the radio channel is not accessible with the frequency domain approach, as mentioned above. Note that even in the time-domain, the time-spreading response is difficult to assess since a full space and time analysis should be done. For a steady-state study, the complexity of both algorithms is comparable.
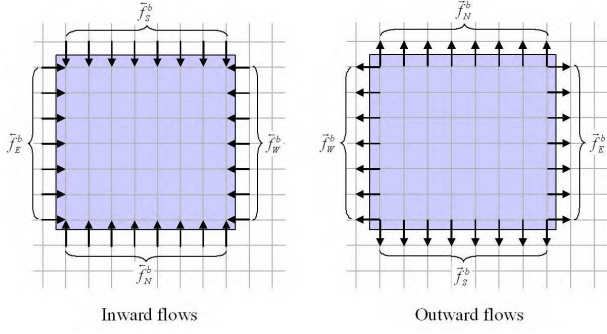
Fig. 2. 4 inward flow vectors (a) and 4 outward flow vectors (b) are associated with each brick.

Fig. 3. the MR-node C is cut into two children MR-node.

C. The MR-node Concept

Let us now introduce the concept of a multi-resolution node (MR-node), comparable to the brick defined by Shlepnev [SHL 01]. The basic idea is the gathering of pixels into rectangular bricks which play the role of a MR-node in a multi-resolution framework. This is a well-used concept in boundary elements methods.

A MR-node, or a brick $B(\overrightarrow{\Delta}, \overrightarrow{P})$ is defined by its size ($\overrightarrow{\Delta} = (\Delta x, \Delta y)$) and the position of its top-left node ($\overrightarrow{p} = (p_x, p_y)$). For each brick, inward and outward flows are defined on its bounds as illustrated in Fig. 2. Each flow is now a vector of size Δ_y or Δ_x respectively for East and West flows and for North and South flows. The propagation over a brick m is now described by :

$$\overrightarrow{F}^b(m) = \Sigma^b(m) \cdot \overleftarrow{F}^b(m)$$

$$\overleftarrow{F}^b(m) = N(\overrightarrow{F}^b(m)) + S^b(m) \tag{12}$$

In order to solve the propagation problem with these bricks, the scattering matrix should be defined according to

$$\Sigma^b(m) = \begin{bmatrix} \sigma^b_{E-E}(m) & \sigma^b_{E-W}(m) & \sigma^b_{E-S}(m) & \sigma^b_{E-N}(m) \\ \sigma^b_{W-E}(m) & \sigma^b_{W-W}(m) & \sigma^b_{W-S}(m) & \sigma^b_{w-N}(m) \\ \sigma^b_{S-E}(m) & \sigma^b_{S-W}(m) & \sigma^b_{S-S}(m) & \sigma^b_{S-N}(m) \\ \sigma^b_{N-E}(m) & \sigma^b_{N-W}(m) & \sigma^b_{N-S}(m) & \sigma^b_{N-N}(m) \end{bmatrix} \tag{13}$$

where for instance $\sigma^b_{N-E}m$ is the part of the scattering matrix which propagates flow $\overleftarrow{f_E^b}$ toward the outward flow $\overrightarrow{f_N^b}$. Therefore, the computation of the wave propagation can be done with these scattering matrices associated with MR-nodes, working with exchange flows only. Algorithm II.1 can be used. In this case, the flows propagate at the speed of a brick instead of a pixel per iteration (with a roughly
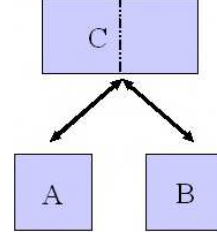
same computation load per iteration). When the steady-state is reached, the inner flows are propagated inside each MR-node independently in each brick (very fast).

III. MULTI-RESOLUTION (MR) APPROACH

A. The Multi-Resolution Recursion

The question remaining in the previous section would be the optimal size of bricks. Instead, we rather introduce a recursive multi-resolution approach which is obtained by gathering bricks into more and more wide bricks until the head node is reached. A formal demonstration of the multi-resolution recursion has been provided in [GOR 03], [GOR 05]. In this paper we rather propose a descriptive way to explain this approach. Let now a MR-node C be settled into two child MR-nodes A and B, according to Fig.3. The inner flows associated with this bloc are no longer all the flows inside the node but only the exchange flows between nodes A and B.

It may be shown that the scattering matrix of MR-node C can be computed from those of its children [GOR 03], [GOR 05], according to

$$\Sigma(C) = U(C) \cdot I(C) \cdot D(C) + f(\Sigma(A), \Sigma(B)) \tag{14}$$

where $f(\Sigma(A), \Sigma(B))$ stands for a linear combination of the sub-matrices $\Sigma(A)$ and $\Sigma(B)$, and $U(C)$, $I(C)$ and $D(C)$ are respectively the upward, the downward, and the inner matrices associated with MR-node C and given by [GOR 05]

$$D(C) = \begin{bmatrix} [0] & \sigma_{WW}(B) & [0] & \sigma_{WS}(B) & [0] & \sigma_{WN}(B) \\ \sigma_{EE}(A) & [0] & \sigma_{ES}(A) & [0] & \sigma_{EN}(A) & [0] \end{bmatrix} \tag{15}$$

and

$$I(C) = \begin{bmatrix} t_{WW}(C) & t_{WE}(C) \\ t_{EW}(C) & t_{EE}(C) \end{bmatrix} \tag{16}$$

with
$$t_{EE}(C) = (I_d - \sigma_{EW}(A) \cdot \sigma_{WE}(B))^{-1},$$

$$t_{WW}(C) = (I_d - \sigma_{WE}(B) \cdot \sigma_{EW}(A))^{-1},$$
$$t_{WE}(C) = \sigma_{WE}(B) \cdot t_{EE}(C),$$
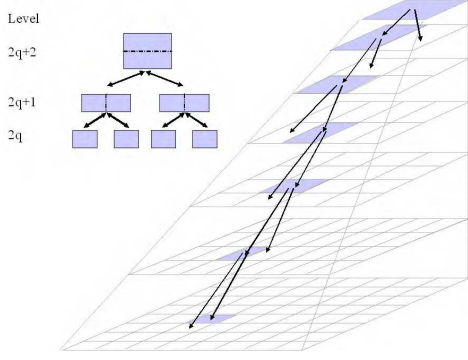$$t_{EW}(C) = \sigma_{EW}(A) \cdot t_{WW}(C).$$

Fig. 4. The regular multi-resolution approach is based on a regular binary tree for assembling MR-nodes.

and

$$U(C) = \begin{bmatrix} [0] & \sigma_{EE}(B) \\ \sigma_{WW}(A) & [0] \\ [0] & \sigma_{SE}(B) \\ \sigma_{SW}(A) & [0] \\ [0] & \sigma_{NE}(B) \\ \sigma_{NW}(A) & [0] \end{bmatrix} \qquad (17)$$

It should be noted that these matrices correspond to a vertical cutting of MR-node C. For an horizontal cutting, these matrices are similar but with permutation of indices E (East) and S (South) in one hand, and of indices W (West) and N (North) in the other hand.

It can be emphasized that only $I(C)$ and $\Sigma(C)$ should be computed and stored for each MR-node, the others pointing directly to parts of its child MR-nodes scattering matrices. A binary tree thus can be built, as described in section III. If the tree is regular, a (ℓ)-level MR-node contains two $(\ell-1)$-level MR-nodes.

The pre-processing phase consists in building this tree structure, and computing the scattering matrices associated with each MR-node.

B. Computing a Source Coverage

Once the binary tree is created and scattering matrices are computed, the propagation can be done in two steps : the upward and the downward. The upward step starts from the source node, and computes the propagation inside its father MR-node. When its outward flows are computed, the father node stands for the new source node. The propagation is then computed in its own father node, and so on until the head node of the binary tree is reached. The two following elementary operations are done in each father of source node

• the steady-state inner flows of father MR-node (C) propagate inside C, as in an isolated world, as illustrated in Fig.6(a). Steady-state flows are then given by

$$\overset{o}{F}(C) = I(C) \cdot \left(\begin{array}{c} \overrightarrow{f_W}(B) \\ \overrightarrow{f_E}(A) \end{array} \right) \qquad (18)$$
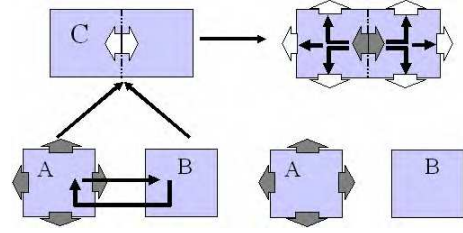

Fig. 5. Upward step. In the left, the MR-node A is a source and Est flow propagates inside C; the steady-state is computed. In the right, the inner flows are propagated to outward flows providing the flows of the MR-node C.
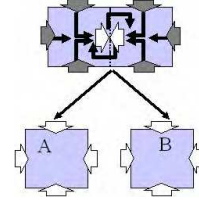

Fig. 6. Downward step. Inward flows of MR-node C propagate inside C leading to inward flows of MR-nodes A and B.

• The second propagates these steady-state inner flows toward outward flows as illustrated in Fig.5(b).

$$\overrightarrow{F}(C) = U(C) \cdot \overset{o}{F}(C) \qquad (19)$$

The downward step implements the propagation of inward flows to inner flows independently in each MR-bloc, according to Fig.6(c) and to

$$\left(\begin{array}{c} \overleftarrow{f_W}(A) \\ \overleftarrow{f_E}(B) \end{array} \right) = D(C) \cdot \overleftarrow{F}(C) + \left(\begin{array}{c} \overrightarrow{f_W}(B) \\ \overrightarrow{f_E}(A) \end{array} \right) \qquad (20)$$

C. Computation Load

The computation load of pre-processing and propagation steps depends on the size of the environment and the size of the larger bricks. It is obvious that for a large enough value of N the fastest approach is obtained by assembling the bricks until the head node is unique. This is the multi-resolution approach. Note however that this is balanced by the need of a pre-processing phase, during which the upward, inner and downward matrices have to be computed. The main computation load of the pre-processing phase is dedicated to the computation of the scattering matrices, which requires one inversion and several multiplications of $N_b x N_b$ matrices, for each brick. The whole computation load is bounded in $O(N^3)$, N being the smaller length of the discrete propagation space. Note that the memory consumption to store all the scattering matrices is in $O(log(N)N^2)$.

The following conclusions may be done :

• The pre-processing computation load is in the order of the minimal computation load that could be achieved with an usual time-domain algorithm while the pre-processing consumes the main computation load. But fortunately, this calculus is done before the source location is defined. This pre-process should be compared to the build of the equivalent source tree in a ray-tracing approach. This approach may be memory consuming although the memory load increases slower than the computation load while the mesh size increases.

• During the propagation phase, a source is propagated (not in a physical sense) upward in the pyramid, and then the inner flows stored in each equivalent source bricks are downward propagated. The computation load is comparable to the computation load of few iterations of the time-domain approach.

• As illustrated in Fig. 4 this method may be used to compute the field in a specific receiver location from a source. In this case the computation time is in $O(N^2)$.

• the final result is the true steady-state.

D. Irregular Tree Building

In the previous section, a tree is built by assembling MR-nodes two by two until the largest brick is built (the whole mesh). This approach leads in fact to a suboptimal gathering process. Indeed, three aims have to be taken into account :

• minimizing the memory consumption

• minimizing the computation load in the pre-processing phase

• minimizing the computation load in the propagation phase

The two former points call for a reduction of the number of brick types. This can be done by trying to have lot of identical bricks in the mesh. The later calls either for a reduction of the number of bricks, or for an approximate evaluation of the field. To answer both points, we propose to build a tree in an irregular manner, in order to favor homogeneous blocs (blocs containing only identical nodes) but under two constraints: a MR-node is always *rectangular* and has always *two children*. An assembling procedure which warrant these conditions until the top of the tree is definitely untractable. It is easier to define instead a downward approach, which consists to divide the head node and its children recursively until the unitary nodes are all reached. This process is illustrated in Fig. 7.

E. The Data Structure

A peculiar data structure has been created to optimize both the memory consumption and the computation load. This structure is illustrated below : The tree of MR-nodes is

Fig. 7. The irregular descendant tree building: the head MR-node is cut along the best discontinuity and so on for its children. The process is herein shown for the head node and "top and left" children recursively.

identified by the head node. Each MR-node has two children and one father. A branch is terminated when a unitary node is reached. Each MR-node is defined by its size and the index of the brick-type it refers to. For instance, an air-filled brick of size NxM. This brick-type is identified in the database and refers to its propagation matrices. Both of these structures are built during the pre-processing phase.

IV. APPLICATION AND RESULTS

A. Indoor Wireless LAN Planning

A software including this approach has been developed for WiFi network planning. The problem is very hardly constrained because :

• The computation should takes less than few minutes to find good Access Point (AP) positions and settings (power, orientation). It means that a full coverage computation should take less than 1 second.

• The typical environment size is about $100m \times 100m$.

• The calculus should run on a standard PC with no more than 1 GO of RAM.

These constraints lead us to consider for the moment only 2D simulations. Furthermore, (5) would imply a very fine discretization step (about $dr = 2cm$ at $f_0 = 2.4GHz$) yielding a typical discrete map about 5000×5000 pixels. The main computation load is devoted to the matrix computations detailed in sectionIII and increases in $0(N^3)$, where N is the smaller environment length. Our experiments have exhibit a wide overhead of computation load and memory consumption if the resolution step is such low. Besides, future norms should use higher frequencies (for instance 5GHz for IEEE802.11a), making unrealistic to achieve reasonable performances at a true frequency. Besides this resolution is much lower than the needed resolution for coverage results. Indeed, the expected accuracy of prediction is rather about one meter. Therefore, our proposal consists in using a simulation frequency, lower than the true frequency, allowing to relax the resolution constraint. Of course, this approximation combined with the 2D formulation and with
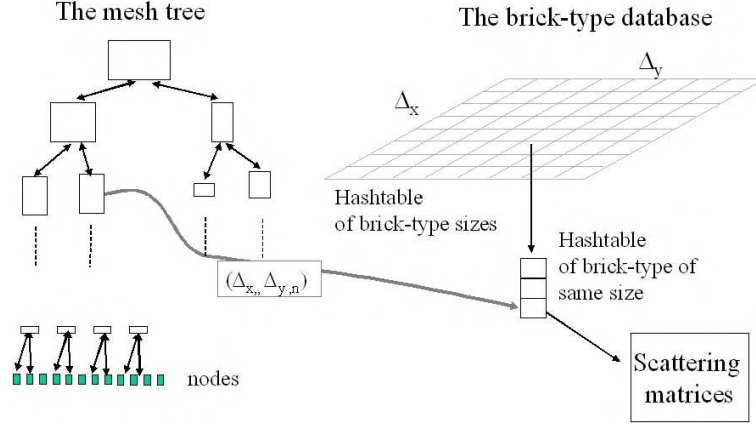
Fig. 8. The data structure contains two main objects : the tree of MR-nodes and the brick types.

the lack of knowledge about building materials and furniture may lead to false predictions. Nevertheless, since reflection coefficients are fixed by the refraction index, they are not frequency dependent. The attenuation law in free space is also independent on the frequency. So, changing the simulation frequency modifies the predictions only in two ways

• The first concerns diffraction at corners. because diffraction is a frequency dependent effect. The use of a lower frequency could under-estimate diffracted waves.

• The second concerns interferences. At each point, the received wave is the sum of several incoming waves. It is obvious that the position of maxima and minima are heavily bounded to the frequency.

In order to reduce the impact of the first, the simulation frequency is chosen such as the simulation wavelength is a multiple of the true wavelength. To overcome the second, the received power is spatially averaged to remove fading. For this purpose, the downward propagation in the pyramid is stopped when homogeneous air-filled nodes are reached. The mean field power is then estimated over this node directly by the following approximation :

$$\overline{|\Psi(\mathbf{m}, \nu_0)|^2} = \sum_{d \in E,W,N,S} \left(\|\overleftarrow{f_d}(m)\|^2 \right) \qquad (21)$$

This approach appeared in fact very efficient for accuracy but also for computation load as described below.

B. Calibration

Due to the previous approximations, it appears easier to use an experimental rather than theoretical calibration process. This experimental calibration uses reference measurements and exploits some parameters in the simulator as weighting parameters. First of all, predictions of the MR-FDPF method are not calibrated in a native way. An offset Δ_Ψ is

introduced. The prediction Ψ_{pred} in decibels (dB) is thus given by:

$$\Psi_{pred} = \Psi_s + \Delta\Psi \qquad (22)$$

where Δ_Ψ is experimentally assessed such as it minimize the RMSE between measured and simulated values. The set of parameters for air and wall constitutive materials α_{air} and (η_k, α_k) are also used to increase the fit between predictions and measurements. This is done by minimizing a least squared criterion with a direct search algorithm called DIRECT presented by Jones et Al. in [JON 93]. Its main advantage is its ability to perform simultaneously a global and a local search. More details are provided in [RUN 05].

C. Experimental Settings

This method has been applied to simulate the field strength inside our lab. The data set includes 200 measurement positions covered by 6 AP's (see [RUN 05]). For each location, about 300 samples per access point were recorded with an 802.11b PCMCIA Orinoco© receiver nested in a laptop. In the simulator, 3 materials were defined: concrete (black), plaster (light grey) and glass (dotted grey) and access points were assumed to be omnidirectional. The calibration has been done with the measurements from one AP and the accuracy has been tested with the others.

D. Results

The coverage prediction at a resolution of 10cm x 10cm (and a simulation frequency of 480MHz) lasts respectively 10sec and 6sec for the pre-processing and the propagation phase. When the propagation is stopped at homogeneous blocs, the propagation time is reduced respectively to 350ms. The corresponding coverage are shown in Fig. 9(a) and (b). The simulations were compared with measurements. Figure 10 shows the simulations (continuous line) and experimental values represented by points (mean values) and their standard deviation (vertical bars). The
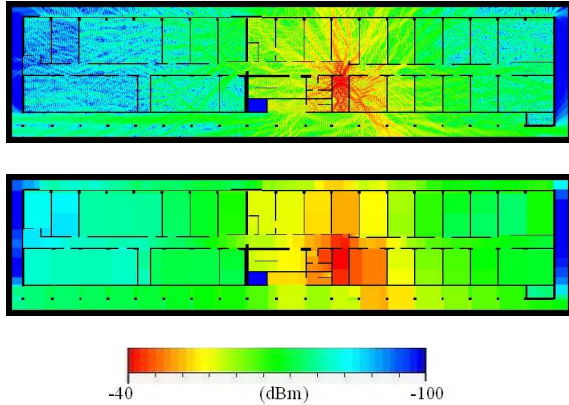
Fig. 9. This figure illustrates the prediction coverage on our lab at two different computation resolutions : (a) unitary nodes of size 10cm x 10cm and (b) homogeneous nodes.
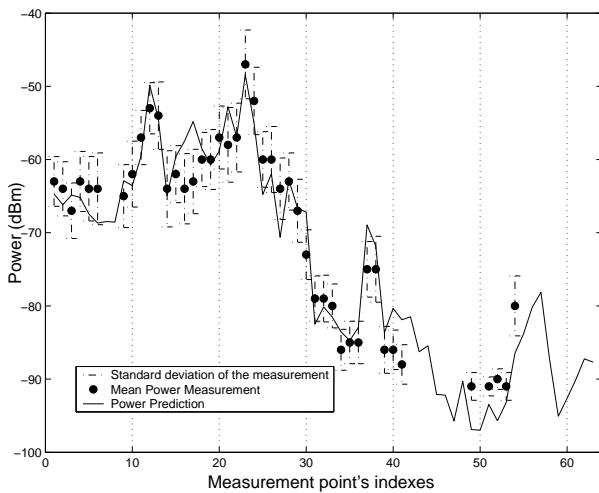

Fig. 10. This figure gives a comparison between experimental and simulated field values along a path in the lab. Black points and vertical bars stand respectively for mean measured power and its standard deviation. The simulation is represented by the continuous line.

simulations obtained after calibration exhibit a mean error about 2dB and a mean standard deviation of less than 4dB. The accuracy of the method is therefore in the order of the stability of the measures.

V. CONCLUSION

The ParFlow method proposed by Luthi for cellular phone systems was rarely used because of the high computation load required for such an approach. The multi-resolution framework developed in the frequency domain allows to reduce drastically this computation load making cense to use this formalism in a 2D Indoor framework. Simultaneously, the accuracy of the approach seems very good despite the fact that the method is in 2D and the simulation frequency was 5 times lower than the real frequency. Further works are concerning three points : reducing the computation load

to permit to work at the true frequency, improving the calibration process, and testing the method in various environments. A very challenging work should be the extension of this approach in a true 3D framework.

REFERENCES

[CHE 97] CHEUNG K., SAU J., R.D.MURCH, *A New Empirical Model Indoor Propagation Prediction*, IEEE Trans. Vehic. Tech., 1997.

[CHO 97] CHOPARD B., LUTHI P., WAGEN J., A lattice boltzmann method for wave propagation in urban microcells, *IEEE Proceedings - Microwaves, Antennas and Propagation*, vol. 144, p. 251–255, 1997.

[GOR 01] GORCE J., UBEDA S., Propagation simulation ith the ParFlow method : fast computation using a multi-resolution scheme., *IEEE 54th Vehicular Technology Conference*, Atlantic City, October 2001.

[GOR 03] GORCE J., JULLO E., RUNSER K., An adaptative multi-resolution algorithm for 2D simulations of indoor propagation, *Proceedings of the 12th International Conference on Antennas and Propagation*, Exeter, UK, IEE, p. 216–219, April 2003.

[GOR 05] GORCE J., RUNSER K., DE LA ROCHE G., The Adaptive Multi-Resolution Frequency-Domain ParFlow (AR-MDPF) method for 2D Indoor radio wave propagation simulation. part I : theory and algorithms., Rapport, INRIA, in press, may 2005.

[HES 02] HESSELBARTH J., VAHLDIECK R., *Accuracy of the frequency-domain TLM method and its application to microwave circuits*, International journal of numerical modelling : electronic networks, devices and fields, vol. 15, p. 371-383, may 2002.

[JOH 87] JOHNS P., *A symmetrical condensed node for the TLM method*, IEEE trans. on Microwave theory Techniques, vol. 35, p. 370-377, 1987.

[JON 93] JONES D., PERTTUNEN C., STUCKMAN B., Lipschitzian Optimization without the Lipschitz Constant, *Journal of Optimization Theory and Applications*, vol. 79, n1, p. 157–181, October 1993.

[LU 04] LU D., RUTLEDGE D., Indoor Wireless Channel Modeling from 2.4 to 24GHz Using a Combined E/H-Plane 2D Ray Tracing Method., *Int. Symp. on Ant. and Prop.*, Monterey, CA., 2004.

[LUT 98] LUTHI P. O., Lattice Wave Automata, PhD thesis, Universit de Genve, Genve, Switzerland, march 1998.

[NES 00] NESKOVIC A., NESKOVIC N., PAUNOVIC G., *Modern approaches in modeling of mobile radio systems propagation environment*, IEEE communication surveys, p. 2-12, 2000.

[REB 99] REBEL J., On the foundation of the transmission Line Matrix Method, PhD thesis, Universitat Munchen, Munchen, Deutchland, dec 1999.

[RUN 05] RUNSER K., GORCE J., Assessment of a new indoor propagation prediction model based on a multi-resolution algorithm, *IEEE Vehicular Technology Conference, spring*, Stockholm, May 2005.

[SHL 01] SHLEPNEV Y., Trefftz-type brick finite elements for electromagnetics, *proc. of the 17 annual review of progress in applied computational electromagnetics*, Monterey, March 2001.

[VAL 93] VALENZUELA R., Ray Tracing approach to predicting indoor wireless transmission., *Proceedings of the 43rd IEEE Vehicular Technology Conference*, p. 214–218, May 1993.